

BULK MINERALOGY OF LUNAR CRATER CENTRAL PEAKS – RESULTS FROM DIVINER LUNAR RADIOMETER. E. Song¹, J.L. Bandfield¹, P.G. Lucey², B.T. Greenhagen³, D.A. Paige⁴. ¹Earth and Space Sciences, University of Washington, eugsong@u.washington.edu, ²Hawaii Institute for Geophysics and Planetology, University of Hawaii at Manoa, ³Jet Propulsion Laboratory, California Institute of Technology, ⁴Department of Earth and Space Sciences, University of California at Los Angeles.

Introduction: The central peaks of lunar impact craters are composed of uplifted material originating from varying depths of the crustal column. Based on the crystallization sequence of the early lunar magma ocean, the anorthositic upper crust becomes progressively more mafic as it approaches the olivine-rich mantle boundary [1]. Previous remote sensing studies have shown that the majority of central peaks within the highlands are highly anorthositic, while more mafic lithologies with greater proportions of olivine and pyroxene are present within maria and large basins [2,3].

Thermal infrared spectra from the Diviner Lunar Radiometer Experiment are used to derive the wavelength location of the Christiansen Feature (CF) that is sensitive to bulk silicate mineralogy [4,5]. A survey of CF values has been performed for the central peaks of 135 complex craters, providing global and regional observations of the heterogeneity of crustal compositions. These results were compared against crustal thickness models [1] and Clementine-derived FeO and optical maturity (OMAT) parameters [6,7].

Data & Methods: The Diviner instrument has 3 spectral bands near $8\mu\text{m}$ that provide the wavelength location of the CF emissivity maximum using the methods from [5]. The CF wavelength position shifts towards shorter wavelengths for anorthositic compositions and longer wavelengths for olivine-rich compositions, with pyroxene falling in-between. Data for this survey were limited to within 30° latitude of the equator and local times between 10:00-14:00 due to anisothermality effects that interfere with the interpretation of the CF [8]. The data are also sensitive to optical maturity, however the degree of weathering is relatively low and uniform on the steeply sloped central peaks so the effect on CF position is minimized. An additional effect that shifts CF position is correlated with temperature and/or solar incidence, but the magnitude of the effect is not symmetrical around local noon. This suggests a dependence on the subsurface thermal gradient which varies relative to the integrated solar insolation received rather than equilibrium temperature.

The magnitude of each of these effects on the CF position has been documented. Data that are severely affected by non-compositional CF shifts were masked out and discarded, particularly in regions where radi-

ance values are transitioning between extremes such as the boundary between a central peak and the crater floor. Data masks were generated to exclude regions where large temperature changes occur over short distances (i.e. dT/dx).

Results: Global. The histogram of CF values from our central peak survey [Fig. 1] shows two maxima at CF values of $8.08\mu\text{m}$ and $8.16\mu\text{m}$ that represent the most frequently occurring peak compositions. The highland and mare crater distributions are skewed towards their respective maxima but are not distinctly split into two populations. The global CF distribution from [5] shows the modal mean CF values for the mare ($8.3\mu\text{m}$) and highlands ($8.15\mu\text{m}$) terrains. The maxima in the central peak CF distribution occur at shorter wavelengths than the global CF distribution, which can be partially attributed to the fact that central peaks tend to be less optically mature than surrounding terrain, which shifts the CF position shortward up to $\sim 0.1\mu\text{m}$.

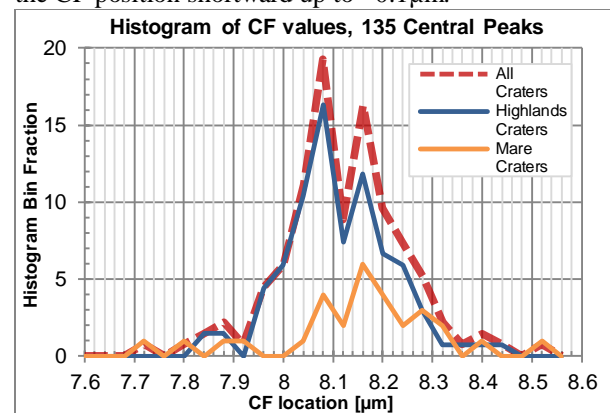


Figure 1. A histogram of CF values from this study, binned in $0.04\mu\text{m}$ increments from $7.6\mu\text{m}$ - $8.56\mu\text{m}$. Dashed line includes all 135 craters, blue and orange lines separate the distribution into craters in the highlands and craters in mare-filled basins.

The similarity between the global CF distribution from [5] and the central peak CF distribution implies that uplifted material found in the central peaks is not significantly different from the range of compositions found on the lunar surface. About 35% of highlands craters and 55% of mare craters have central peaks with CF values between $8.15\mu\text{m}$ and $8.3\mu\text{m}$, indicating that much of the uplifted material has mafic compositions with similar plagioclase to mafic ratios as mare basalts, regardless of surface terrain. Central peak CF values are correlated strongly with Clementine-derived

FeO abundance, but largely independent of regional crustal thickness and the central peak depth of origin [method from 3].

Regional Results. Out of the 135 craters surveyed, 6 craters exhibit central peak compositions more mafic than average maria, with CF values greater than $8.3\mu\text{m}$. Clementine-derived FeO abundances for these craters are between 9-15% vol. Three of these craters are located in the mare, with the highest CF value from the survey - $8.48\mu\text{m}$ - located in the central peaks of Eratosthenes crater in Mare Imbrium [Fig. 2]. The CF value map [Fig.2] shows that the mafic exposure on the central peak of Eratosthenes is broad and sustained on both north and south-facing slopes, indicating that the CF position is unaffected by temperature-dependent anomalies.

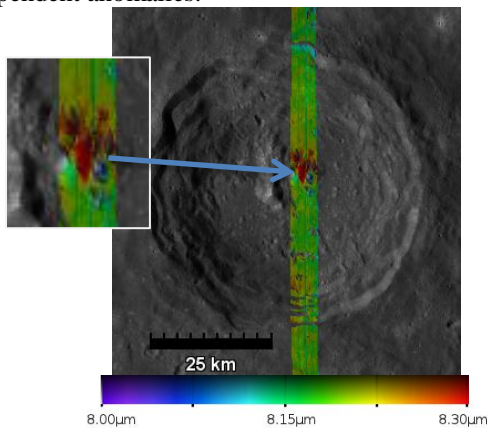


Figure 2. Eratosthenes crater CF value overlay on LROC WAC basemap. Note the broad extent of the high CF feature on the central peak. CF map stretched from 8.0-8.3 μm .

Two of the highlands craters with high CF values - Plummer and Barringer craters - are located along the northern rim of South Pole-Aitken Basin with CF values of $8.42\mu\text{m}$ and $8.36\mu\text{m}$, respectively. Taruntius and Gutenberg craters (central peak CF values of $8.39\mu\text{m}$ and $8.31\mu\text{m}$) are located in the nearside maria surrounding Fecundiatis Basin. Scaliger crater in the far-side highlands has an average CF value of $8.39\mu\text{m}$ in its central peak.

Copernicus crater [Fig. 3], which has been reported in previous works to contain exposures of pure olivine in its central peaks [2,3,9 among others], shows an average CF value of $8.14\mu\text{m}$ at its center-most peak, consistent with an anorthosite-rich composition with small amounts of olivine mixed in. The northern crater wall, however, shows a $\sim 4\text{km}$ long exposure of more mafic material with an average CF value of $8.33\mu\text{m}$.

Aristarchus and Kepler craters, both in the nearside Procellarum basin, exhibited the two lowest CF values found in this study of $\sim 7.7\mu\text{m}$ and $7.79\mu\text{m}$. The highly silicic compositions of the Aristarchus crater region [10] have CF wavelengths that are too short to be re-

solved with the Diviner bands, so its CF value is approximate.

Conclusion: This study has identified 6 craters with central peak compositions that are more mafic than mare basalt, however none of these craters exhibit CF values indicative of ultra-mafic mantle-sourced material. Most of the uplifted mafic material from this survey shows a silicate composition with a mafic component similar to mare basalt, which could be sourced from mafic plutons or cryptomaria. The wide variety of compositions found in mare crater central peaks, including the craters with the highest and lowest CF values on the Moon, indicates a great deal of inhomogeneity in the lunar crust.

Lack of correlations, particularly to crust thickness, could be due to the complex cratering history that constantly overturned the original crust's stratigraphy. A possible scenario is that the impacts included in this study have uplifted previously overturned stratigraphy, so the stratigraphic sequence exposed in central peaks may be incoherently inverted.

References: [1] Wieczorek, M.A. et al (2006) *Rev. Mineral. Geochem.*, 60, 221-364. [2] Tompkins, S. and Pieters, C.M. (1997) *Meteorit. Planet. Sci.*, 34, 25-41. [3] Cahill, J.T.S. et al (2009) *J. Geophys. Res.*, 114, 1-17. [4] Salisbury, J.W. and Walter, L.S. (1989) *J. Geophys. Res.*, 94, 9192-9202. [5] Greenhagen, B.T. et al (2010), *Science*, 329, 1507-9. [6] Lucey, P.G. et al (1998) *LPS XXIX*, 1356-1357. [7] Lucey, P.G. et al (1995) *Science*, 268, 1150-3. [8] Bandfield, J.L. (2009) *Icarus*, 202, 414-428. [9] Yamamoto, S. et al (2010), *Nat. Geosci.*, 3, 533-6. [10] Glotch, T.D. et al (2010), *Science*, 328, 1510-3.

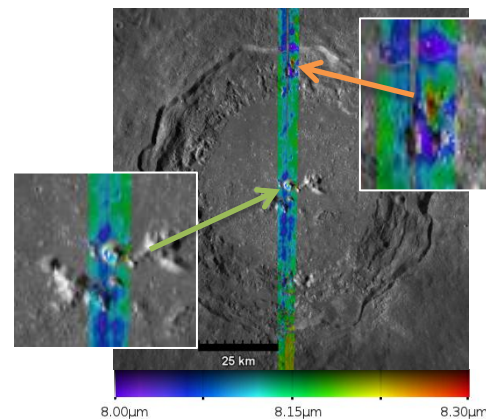


Figure 3. Copernicus crater CF value overlay on LROC WAC basemap. Note that much of the CF data in the central peak region is masked out due to anisothermality-related effects which overwhelm any CF shifts due to compositional variation. The northern crater wall shows a vertical smudge-like high CF feature that is sustained across $\sim 4\text{km}$.